Transp Porous Med (2011) 87:41–48
DOI 10.1007/s11242-010-9712-7

Note on the "Scaling Transformations for Boundary Layer Flow near the Stagnation-Point on a Heated Permeable Stretching Surface in a Porous Medium Saturated with a Nanofluid and Heat Generation/ Absorption Effects"

Eugen Magyari

Received: 14 December 2010 / Accepted: 30 December 2010 / Published online: 12 January 2011

Abstract In a recent paper by Hamad and Pop (Transp Porous Med 2010) a comprehensive numerical study of the title problem has been reported. The goal of the present note is (i) to give exact analytical solutions of this model for some special cases of physical interest, and (ii) to point out that within the model considered by Hamad and Pop no essential distinguishing features between the convective heat transfer in nanofluids and in usual viscous fluids occur.

Keywords Porous media · Nanofluids · Stretching surfaces · Stagnation-point flow · Exact solutions

1 Introduction and Problem Formulation

In a recent paper by Hamad and Pop (2010), the steady plane stagnation-point flow in a nanofluid saturated porous medium has been investigated. The permeable plane surface was stretched in two opposite directions with a velocity proportional to the surface coordinate x, keeping the origin fixed. Both the surface temperature T_w and the ambient temperature T_∞ of the nanofluid are constant. It was assumed that the base fluid (water) and the nanoparticles (Cu, Al_2O_3, TiO_2) are in thermal equilibrium and no slip occurs between them. In the energy balance, the effect of a volumetric heat generation or absorption has been included assuming that its intensity is proportional to the local temperature difference $T - T_\infty$. The governing dimensional boundary layer equations and the corresponding boundary conditions have been written in the form (Hamad and Pop 2010)

$$\frac{\partial \bar{u}}{\partial \bar{x}} + \frac{\partial \bar{v}}{\partial \bar{y}} = 0 \tag{1}$$

E. Magyari (✉)
Departement Physik, Universität Basel, Klingelbergstr. 82, 4056 Basel, Switzerland
e-mail: magyari@bluewin.ch

$$\bar{u}\frac{\partial \bar{u}}{\partial \bar{x}}+\bar{v}\frac{\partial \bar{u}}{\partial \bar{y}}=\bar{U}\left(\bar{x}\right)\frac{d\bar{U}\left(\bar{x}\right)}{d\bar{x}}+\frac{\mu_{\rm nf}}{\rho_{\rm nf}}\frac{\partial^2\bar{u}}{\partial \bar{y}^2}+\frac{\mu_{\rm nf}}{\rho_{\rm nf}K}\left(\bar{U}\left(\bar{x}\right)-\bar{u}\right) \tag{2}$$

$$\bar{u}\frac{\partial T}{\partial \bar{x}}+\bar{v}\frac{\partial T}{\partial \bar{y}}=\alpha_{\rm nf}\frac{\partial^2 T}{\partial \bar{y}^2}+\frac{Q_0}{\left(\rho C_p\right)_{\rm nf}}\left(T-T_\infty\right) \tag{3}$$

$$\bar{u}=\bar{u}_{\rm w}\left(\bar{x}\right)=cx,\ \bar{v}=\bar{v}_{\rm w},\ T=T_{\rm w}\quad \text{on } \bar{y}=0 \tag{4}$$

$$\bar{u}\to\bar{U}\left(\bar{x}\right)=ax,\ T\to T_\infty\quad \text{as } \bar{y}\to\infty \tag{5}$$

In the above equations, all the symbols have the usual meaning and the subscript nf stands for "nanofluid". After a nondimensionalization, the subsequent introduction of a stream function ψ and the usual similarity transformation for the plane stagnation-point flows, $\psi=xF\left(\eta\right),\ \eta=y$, the boundary value problem (15) has been reduced to the form (Hamad and Pop 2010)

$$F'''+K_1\left(\frac{a}{c}-F'\right)+\left(1-\phi\right)^{2.5}\left(1-\phi+\phi\frac{\rho_{\rm s}}{\rho_{\rm f}}\right)\left(FF''-F'^2+\frac{a^2}{c^2}\right)=0 \tag{6}$$

$$\frac{\alpha_{\rm nf}}{\alpha_{\rm f}}\frac{1}{Pr}\theta''+F\theta'+\frac{\lambda}{1-\phi+\phi\frac{\left(\rho C_p\right)_{\rm s}}{\left(\rho C_p\right)_{\rm f}}}\theta=0 \tag{7}$$

$$F\left(0\right)=S,\quad \mathrm{F}'\left(0\right)=1,\quad \mathrm{F}'\left(\infty\right)=a/c \tag{8}$$

$$\theta\left(0\right)=1,\quad \theta\left(\infty\right)=0 \tag{9}$$

where the primes denote differentiations with respect to η, $K_1=\nu_{\rm f}/\left(cK\right)$ is the permeability parameter, $\lambda=Q_0/\left(c\rho C_{\rm pf}\right)$ the heat generation/absorption parameter, $Pr=\nu_{\rm f}/\alpha_{\rm f}$ the Prandtl number of the base fluid, $S=-\bar{v}_{\rm w}/\sqrt{c\nu_{\rm f}}$ the suction/injection parameter, ϕ stands for the volume fraction of the nanoparticles in the nanofluid, the subscript f refers to the base fluid and s to the solid nanoparticles (for the detailed expressions of the material constants involved in the present problem see Eq. 5 of Hamad and Pop 2010). In the paper of Hamad and Pop (2010), the influence of the characteristic parameters on the flow and heat transfer features of nanofluids has been investigated numerically in some detail. For the sake of an analytical progress in this new research field, in this article exact solutions will be presented for the values 1 and 0 of the velocity ratio $r\equiv a/c$ of the inviscid free stream and the wall motion.

2 Exact Solutions for $a=c$

For $a=c$, the velocity ratio $r\equiv a/c$ is 1 which means that the surface velocity $\bar{u}_{\rm w}\left(\bar{x}\right)=cx$ equals the stagnation point velocity $\bar{U}\left(\bar{x}\right)=ax$ in the inviscid free stream. It is immediately seen that in this case Eq. 6 admits the simple solution

$$F=S+\eta \tag{10}$$

which satisfies all the boundary conditions (8). Accordingly, the similar velocity $F'\left(\eta\right)$ is constant, $F'\left(\eta\right)=1$, and the corresponding dimensionless velocity field $\left(u,v\right)=\left(x,-y-S\right)$ coincides with the velocity of the potential flow in the neighborhood of the stagnation point. The temperature equation Eq. 7 reduces to

$$\frac{1}{Pr_1}\theta''+\left(S+\eta\right)\theta'+\lambda_1\theta=0 \tag{11}$$

where the following short notations were used

$$Pr_1 = \frac{\alpha_{\rm f}}{\alpha_{\rm nf}} Pr, \quad \lambda_1 = \lambda \left(1 - \phi + \phi \frac{(\rho C_p)_{\rm s}}{(\rho C_p)_{\rm f}} \right)^{-1} \tag{12}$$

Introducing the new independent variable

$$\xi = \sqrt{\frac{Pr_1}{2}} (S + \eta) \tag{13}$$

Equation 11 becomes

$$\frac{{\rm d}^2\theta}{{\rm d}\xi^2} + 2\xi \frac{{\rm d}\theta}{{\rm d}\xi} + 2\lambda_1 \theta = 0 \tag{14}$$

The boundary value problem (14), (9) admits closed form solutions in several special cases of physical interest. The most simple solution is obtained in the case of volumetric heat generation with $\lambda_1 = 1$. This solution $\theta(\eta)$ and the corresponding wall temperature gradient $\theta'(0)$ read

$$\theta(\eta) = e^{\xi_0^2 - \xi^2} = e^{-\frac{1}{2} Pr_1 (\eta^2 + 2S\eta)}, \quad \theta'(0) = -Pr_1 S \quad (\lambda_1 = 1) \tag{15}$$

The basic features of the solution (15) are illustrated in Fig. 1 for an impermeable surface ($S = 0$) and a permeable surface with lateral suction ($S = +0.3$, blue curve) and lateral injection ($S = -0.3$, red curve) of the nanofluid. In the latter case, an overshooting temperature profile occurs which reaches the maximum value $\theta_{\max} = \exp\left(Pr_1 S^2/2\right) = 1.2523$ at $\eta = -S = 0.3$. The heat flux is reversed in this case, the heat being transferred from the fluid to the surface. The impermeable surface ($S = 0$, green curve) on the other hand, is adiabatic, $\theta'(0) = 0$.

In the absence of the heat sources and sinks, $\lambda = 0$, as well as in the presence of volumetric heat absorption (consumption), $\lambda < 0$, the solution can be given in terms of the *repeated integrals of the complementary error function* (see e.g., Abramowitz and Stegun 1972, Chap. 7) assuming that λ_1 is, respectively, zero or a negative integer, $\lambda_1 = -n$, $n = 0, 1, 2, 3, \ldots$. In these cases, one has

$$\theta(\eta) = \frac{{\bf i}^n {\rm erfc}\,(\xi)}{{\bf i}^n {\rm erfc}\,(\xi_0)} \quad (\lambda_1 = -n) \tag{16}$$

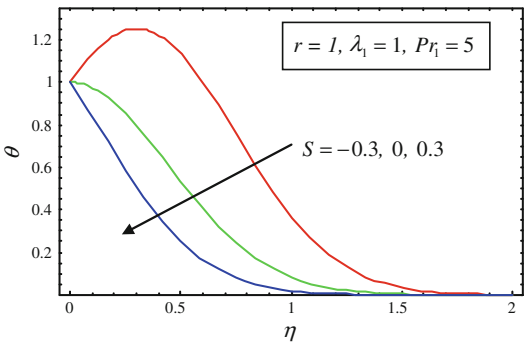

Fig. 1 Temperature profiles in the presence of heat generation with $\lambda_1 = 1$. In the case of lateral injection of the nanofluid (*red curve* $S = -0.3$) a temperature overshoot occurs, while the impermeable surface (*green curve* $S = 0$) is adiabatic, $\theta'(0) = 0$

where

$$\xi_0 = \xi|_{\eta=0} = \sqrt{\frac{Pr_1}{2}}S \tag{17}$$

The corresponding wall temperature gradient is

$$\theta'(0) = -\frac{\mathbf{i}^{n-1}\mathrm{erfc}\,(\xi)}{\mathbf{i}^{n}\mathrm{erfc}\,(\xi_0)}\sqrt{\frac{Pr_1}{2}} \quad (\lambda_1 = -n) \tag{18}$$

In case $\lambda_1 = 0$ (absence of the heat sources and sinks), Eqs. 16 and 18 reduce to

$$\theta(\eta) = \frac{\mathrm{erfc}\,(\xi)}{\mathrm{erfc}\,(\xi_0)}, \quad \theta'(0) = -\frac{\exp\left(-\xi_0^2\right)}{\mathrm{erfc}\,(\xi_0)}\sqrt{\frac{2Pr_1}{\pi}} \quad (\lambda_1 = 0) \tag{19}$$

and in case $\lambda_1 = -1$ (volumetric heat absorption) to

$$\begin{aligned}\theta(\eta) &= \frac{exp\left(-\xi^2\right) - \sqrt{\pi}\xi\,\mathrm{erfc}\,(\xi)}{\exp\left(-\xi_0^2\right) - \sqrt{\pi}\xi_0\mathrm{erfc}\,(\xi_0)},\\ \theta'(0) &= -\frac{(\pi\, Pr_1/2)^{1/2}\,\mathrm{erfc}\,(\xi_0)}{\exp\left(-\xi_0^2\right) - \sqrt{\pi}\xi_0\mathrm{erfc}\,(\xi_0)}\end{aligned} \quad (\lambda_1 = -1) \tag{20}$$

In Fig. 2a, the temperature profiles (19) with $\lambda_1 = 0$ have been plotted for $Pr_1 = 3$ and three different values of the transpiration parameter S, and in Fig. 2b the negative wall

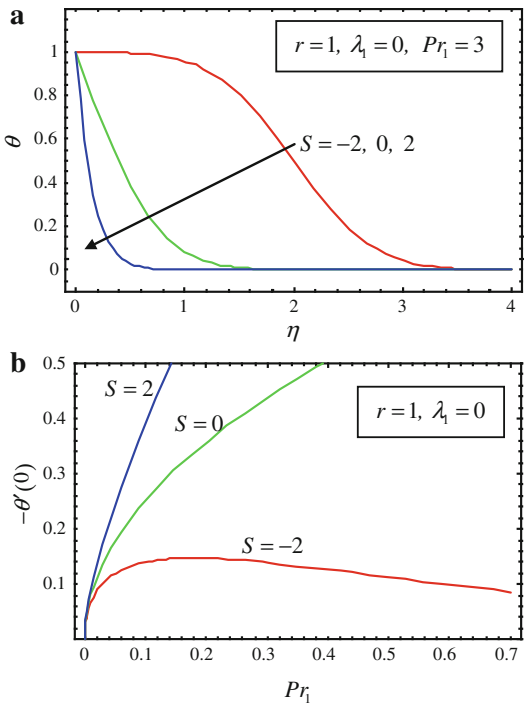

Fig. 2 **a** Temperature profiles in the absence of heat sources and sinks ($\lambda_1 = 0$) for $Pr_1 = 3$ and the indicated values of the transpiration parameter S. **b** The negative wall temperature gradients $-\theta'(0)$ corresponding to $\lambda_1 = 0$ and $S = -2,\ 0,\ 2$ plotted as functions of the modified Prandtl number Pr_1

temperature gradients $-\theta'(0)$ corresponding to the respective values $S = -2,\ 0,\ 2$ of S are shown as functions of the modified Prandtl number Pr_1. For small values of Pr_1, all three functions $-\theta'(0)$ scale as $\sqrt{2Pr_1/\pi}$, but for increasing values of Pr_1 different behaviors occur. While the blue and green curves corresponding, respectively, to $S = 2$ and $S = 0$ are steeply and monotonically ascending, the red curve corresponding to the lateral injection of the nanofluid with $S = -2$ reaches at $Pr_1 = 0.1764$, the maximum value $-\theta'(0) = 0.1473$ and then decreases and approaches zero as $Pr_1 \to \infty$. Such a behavior of $-\theta'(0)$ in convective heat transfer is unusual.

The case $\lambda_1 = -1$ (heat absorption) is illustrated in Fig. 3a, where the temperature profiles (20) have been plotted for $Pr_1 = 5$ and three different values of the transpiration parameter S. In this case, in contrast to heat generation case plotted in Fig. 1, no temperature overshoot occurs for $S < 0$. In Fig. 3b, the negative wall temperature gradients $-\theta'(0)$ corresponding to the respective values $S = -1,\ 0,\ 1$ of S are shown as functions of the modified Prandtl number Pr_1. For small values of Pr_1, all three functions $-\theta'(0)$ scale as $\sqrt{\pi\, Pr_1/2}$, but for increasing values of Pr_1 different behaviors occur also in this case. While the blue and green curves corresponding respectively to $S = 1$ and $S = 0$ are steeply ascending, the red curve corresponding to the lateral injection of the nanofluid with $S = -1$ approaches the value 1 as $Pr_1 \to \infty$.

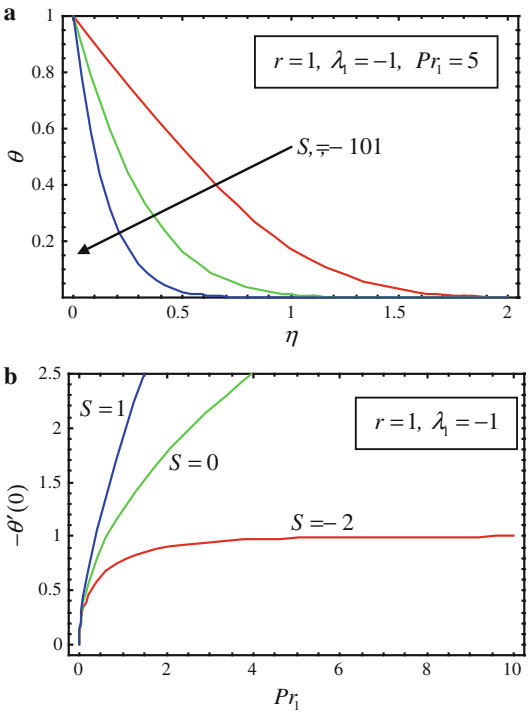

Fig. 3 **a** Temperature profiles in the presence of heat absorption with $\lambda_1 = -1$ for $Pr_1 = 5$ and the indicated values of the transpiration parameter S. **b** The negative wall temperature gradients $-\theta'(0)$ corresponding to $\lambda_1 = -1$ (heat absorption) and $S = -1, 0, 1$ plotted as functions of the modified Prandtl number Pr_1

3 Exact Solutions for $a = 0$

When $a = 0$, i.e., $r = 0$, the flow is driven only by the wall which is stretching with the linearly rising velocity $\bar{u}_w(\bar{x}) = cx$. Therefore, this flow configuration is the porous-medium counterpart of the classical *Crane flow* of a clear viscous fluid. In this case, the flow boundary value problem (6), (8) reduces to

$$F''' - K_1 F' + \gamma \left(FF'' - F'^2\right) = 0 \tag{21}$$

$$F(0) = S, \quad F'(0) = 1, \quad F''(\infty) = 0 \tag{22}$$

where the short notation

$$\gamma = (1-\phi)^{2.5}\left(1 - \phi + \phi\frac{\rho_s}{\rho_f}\right) \tag{23}$$

has been used.

The boundary value problem (21), (22) admits the exact solution

$$F(\eta) = S + \frac{1}{b}\left(1 - e^{-b\eta}\right) \tag{24}$$

where

$$b = \frac{1}{2}\left(\gamma S + \sqrt{\gamma^2 S^2 + 4(\gamma + K_1)}\right) > 0 \tag{25}$$

Thus, the dimensionless wall shear stress is $F''(0) = -b$ and the temperature Eq. 7 becomes

$$\frac{1}{Pr_1}\theta'' + \left(S + \frac{1}{b} - \frac{e^{-b\eta}}{b}\right)\theta' + \lambda_1\theta = 0 \tag{26}$$

Changing from η and θ to the new variables z and w defined as

$$z = -\frac{Pr_1}{b^2}e^{-b\eta}, \quad \theta = z^{a_1}w(z) \tag{27}$$

Equation (26) goes over in

$$z\frac{\mathrm{d}^2 w}{\mathrm{d}z^2} + (b_1 - z)\frac{\mathrm{d}w}{\mathrm{d}z} - a_1 w = 0 \tag{28}$$

where

$$b_1 = 1 + 2a_1 - \frac{Pr_1}{b^2}(1 + bS) \tag{29}$$

and a_1 satisfies the quadratic equation

$$a_1^2 - \frac{Pr_1}{b^2}(1 + bS)\,a_1 + \frac{Pr_1\lambda_1}{b^2} = 0 \tag{30}$$

The solutions of the boundary value problem (26), (9) can be given in this case in terms of Kummer's confluent hypergeometric function $M(a, b; z)$ (see e.g., Abramowitz and Stegun 1972, Chap. 13) as

$$\theta(\eta) = e^{-ba_1\eta}\frac{M\left(a_1, b_1; -\frac{Pr_1}{b^2}e^{-b\eta}\right)}{M\left(a_1, b_1; -\frac{Pr_1}{b^2}\right)} \tag{31}$$

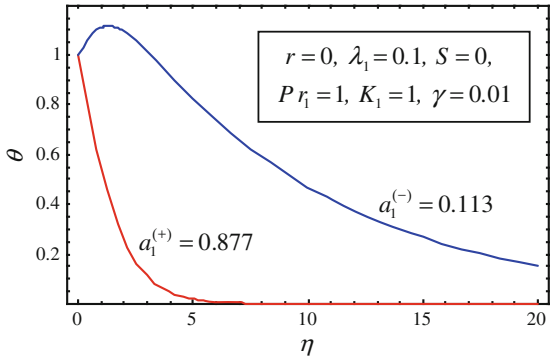

Fig. 4 Dual temperature profiles corresponding to the two positive roots of the quadratic Eq. 30 for the indicated values of the parameters. In this case, $b = 1.005$

The wall temperature gradient corresponding to the solution (31) is

$$\theta'(0) = -ba_1 + \frac{a_1 Pr_1}{b_1 b} \frac{M\left(a_1+1, b_1+1; -\frac{Pr_1}{b^2}\right)}{M\left(a_1, b_1; -\frac{Pr_1}{b^2}\right)} \tag{32}$$

A comprehensive discussion of the structure of solution space specified by Eq. 31 for various values of the parameters λ_1, S, Pr_1, K_1, and γ exceeds the framework of the present note. On this reason, only two essential features will be mentioned here. One of these features is that in the case when Eq. 30 admits two positive roots,

$$a_1^{(\pm)} = \frac{Pr_1}{2b^2}(1+bS)\left[1 \pm \sqrt{1 - \frac{4\lambda_1 b^2}{Pr_1(1+bS)^2}}\right] > 0 \tag{33}$$

equation 31 furnishes dual solutions which correspond to $a_1 = a_1^{(+)}$ and $a_1 = a_1^{(-)}$, respectively. This property is illustrated in Fig. 4 where dual solutions are shown for the indicated values of the parameters involved. The corresponding roots $a_1^{(+)} = 0.877$ and $a_1^{(-)} = 0.113$ are associated with a rapidly and a slowly decaying temperature profile, respectively. In the latter case, also a temperature overshoot occurs. The second important property of the solutions (31) is that in the range $S > -1/b$ and in the absence of heat generation and absorption, $\lambda_1 = 0$, which is the case of the main practical interest, the solution is always unique and corresponds to the root $a_1^{(+)} = Pr_1(1+bS)/b^2 > 0$ of Eq. 30.

4 Comments on the Present Nanofluid Model

The aim of this section is to compare the present *nanofluid model* specified by Eqs. 6–9 of Hamad and Pop (2010) to the flow and heat transfer model of a *usual viscous fluid* under the same physical conditions. To this end, it is convenient to first rescale Eqs. 6–9 according to the transformations

$$f(\xi) = \sqrt{\gamma} F(\eta), \quad \xi = \sqrt{\gamma}\eta \tag{34}$$

where γ is specified by Eq. 23. Under the transformations (34), which represent a stretching of the old dependent and independent variables F and η by the same factor $\sqrt{\gamma}$, Eqs. 6 and 7 go over in

$$\dddot{f} + \tilde{K}\left(\frac{a}{c} - \dot{f}\right) + f\ddot{f} - \dot{f}^2 + \frac{a^2}{c^2} = 0 \tag{35}$$

$$\frac{1}{\tilde{Pr}}\ddot{\theta} + f\dot{\theta} + \lambda_1\theta = 0 \tag{36}$$

where $\tilde{K} = K_1/\gamma$, $\tilde{Pr} = Pr_1/\gamma$, Pr_1 and λ_1 are given by Eq. (12), and the dots denote differentiations with respect to ξ. The boundary conditions (8) and (9) become

$$\begin{aligned} &f(0) = \tilde{S}, \quad \dot{f}(0) = 1, \quad \dot{f}(\infty) = a/c, \\ &\theta(0) = 1, \quad \theta(\infty) = 0 \end{aligned} \tag{37}$$

where $\tilde{S} = S\sqrt{\gamma}$.

Now, in the limiting case of vanishing volume fraction of the nanoparticles, $\phi \to 0$, one has $\gamma \to 1$, $\tilde{K} \to K_1$, $\alpha_{nf} \to \alpha_{\mathrm{f}}$, $\tilde{Pr} \to Pr_1 \to Pr$, $\lambda_1 \to \lambda$ and $\tilde{S} \to S$. This means that within the present model, no distinguishing features between the nanofluids and the usual viscous fluids occur. The only difference consists in the numerical values of the parameters present in the basic Eqs. 35–37. In other words, the behavior of a nanofluid within the model considered by Hamad and Pop (2010) is exactly the same as the behavior of a usual viscous (base) fluid with changed thermophysical properties. Obviously, this feature becomes manifest already in the dimensional Eqs. 1–5 where none of the two fundamental effects of the nanofluid convective heat transfer, namely the *Brownian diffusion* and the *thermophoretic diffusion* (see e.g., Buongiorno 2006) has been included.

5 Conclusion

The convective nanofluid heat transfer models which do not include the two main velocity slip effects of the nanoparticles with respect to the base fluid, namely the *Brownian diffusion* and the *thermophoretic diffusion* are essentially equivalent to the corresponding viscous flow models for the base fluid.

References

Abramowitz, M., Stegun, I.A.: Handbook of Mathematical Functions. Dover, New York (1972)
Buongiorno, J.: Convective transport in nanofluids. ASME J. Heat Transf. **128**, 240–250 (2006)
Hamad, M.A.A., Pop, I.: Scaling transformations for boundary layer flow near the stagnation-point on a heated permeable stretching surface in a porous medium saturated with a nanofluid and heat generation/absorption effects. Transp. Porous Med. (2010). doi:10.1007/s11242-010-9683-8